Hand Exoskeleton for Rehabilitation and Functionalization

Tiago Leite [1], Eurico Seabra [1]

[1] *MEtRICs - Centre for Mechanics and Materials Technologies and Unit of Environmental Biotechnology - Department of Mechanical Engineering, School of Engineering, University of Minho, Campus de Azurém, 4800-058 Guimarães, Portugal*

Abstract

Many diseases and injuries of the hand require rehabilitation to restore function. However, the high human, financial, spatial, and temporal costs associated with rehabilitation often mean that the population in need does not have access to optimal rehabilitative care. Therefore, devices that complement the therapist are a possible solution, as they make rehabilitation more independent and frequent, and save healthcare facilities the aforementioned resources. Nevertheless, these devices are not widely distributed in the market, mainly due to their poor accessibility. The newly designed exoskeleton has four motors and a redundant transmission system that allows independent flexion and extension of each finger, except the thumb. Kinematics were analyzed with motion studies and loads were evaluated with static studies and structural analysis using motion loads. In the simulations, both flexion and extension were achieved in four seconds. A prototype transmission system was built and its kinematics matched that of the simulation and corresponded to the biomechanics of the fingers. At maximum flexion, the exoskeleton would be able to hold small objects and exert a normal force of up to 20 N with structural integrity.

Keywords

Engineering design, exoskeleton, hand rehabilitation, hand functionalization.

1. Introduction

The hand played a prominent role in human evolution. Through anatomical changes, the main function of the hand shifted from locomotion to object handling, communication, and sociocultural interactions. Most of our daily activities depend on the hand, which means that quality of life declines when this complex and versatile organ is impaired.

According to the American Society of Plastic Surgeons, hand surgery was among the top five reconstructive procedures performed in 2020 [1], and this number is predicted to increase in the future [2]. It could be concluded that the need for hand rehabilitation after surgery will follow this trend. In addition, other conditions such as strokes and spinal cord injuries further increase the need for rehabilitation and functionalization of the hand.

Hand exoskeletons offer rehabilitation that focuses on repeatability and automation, allowing data collection and gamification, among others. This saves healthcare resources while improving patient management and monitoring, which is critical given the increasing pressure on healthcare facilities and professionals [3]. The use of exoskeletons provides the potential for independent and remote rehabilitation where patients are only monitored by healthcare professionals. The same caregiver could monitor multiple patients simultaneously or prescribe a plan with a series of programmed movements.

Although research on hand exoskeletons continues to advance, few are marketed, and even these are intended for use in clinical settings [4] and are prohibitively expensive for most people. On this basis, the need for wearable exoskeletons at moderate prices and that allow independent rehabilitation becomes apparent.

1.1. Biomechanical overview

The hand and wrist consist of the radius and ulna, eight carpals (divided into two rows), five

EMAIL: tiago.costa.leite@outlook.pt (A. 1);
eseabra@dem.uminho.pt (A. 2);
ORCID: 0000-0002-1728-2839 (A. 2);

metacarpals, and 14 phalanges (three in each finger, except the thumb with only two).

The muscles of the hand are divided into extrinsic and intrinsic. The former are located outside the hand and insert into it, while the latter are located inside the hand. This division places the contractile part of some muscles, which have a greater volume, outside the hand, allowing finer movements. Both muscle groups together are responsible for actuating all degrees of freedom of the hand. The most important movements of the hand and wrist are [5]:

- supination, pronation, abduction, adduction, flexion, and extension of the wrist;
- flexion, extension, abduction, adduction, opposition, and reposition of the thumb;
- flexion, extension, abduction, and adduction of the index, middle, ring, and little fingers;
- minor movements of the carpometacarpal and intermetacarpal joints.

1.2. Hand Exoskeleton Modules

Hand exoskeletons can be divided into several modules. Following Bos et al. (2016) [4], the modules actuation, motion transmission, and control have been defined.

Most exoskeletons use electric motors, such as linear actuators and servo motors. However, other options are less commonly used: pneumatic (pneumatic muscles or pistons) and hydraulic actuators, shape memory alloys, active polymers, body-driven actuation, and others [4,6].

Motion can be transmitted directly through the actuators (e.g., pneumatic muscles), through tendon-like systems (e.g., with cables), and through rigid mechanisms (matched-axis, remote centers of rotation, redundant linkage, and base-to-distal). This module is often used as a strategy for underactuation, reducing overall cost, volume, and weight. The rigid mechanisms provide better trajectory control and lower variability but are usually larger than non-rigid transmission [4,7].

Finally, as far as finger control is concerned, it can range from fully passive (the movement is performed entirely by the exoskeleton) to fully active (the movement is performed exclusively by the user, but the exoskeleton defines the trajectory and has mainly a monitoring function). The trigger for the movements can be done in many ways, highlighting EMG and EEG in more complex systems or buttons and pre-programmed movement plans in simpler systems [8].

2. Exoskeleton Design

Initially, a hand model was developed based on average male measurements from an anthropometric study of 2307 US Army personnel [9].

Although the kinematics of the model are much simpler than those of a real hand, the model provides a basis for testing the exoskeleton and for articulating the degrees of freedom of flexion and extension of each of the phalangeal joints.

The next step was to design the attachments to the fingers and dorsal region (Figure 1). These elements can be 3D printed and attached to the hand with hook and loop straps, resulting in low overall production costs.

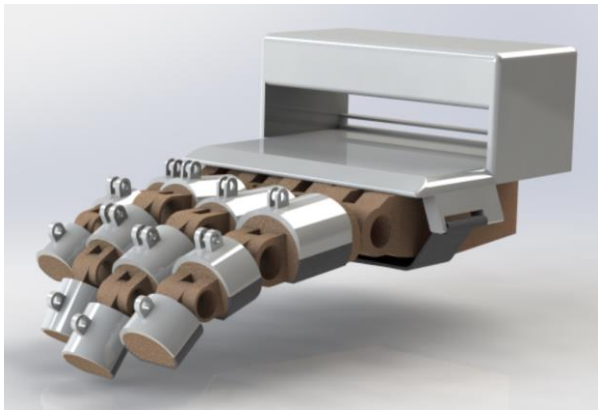

Figure 1: 3D model of the hand, the supports, and the straps

The motion transmission was achieved using a newly developed redundant bar linkage (Figure 2). This type of linkage offers a certain degree of adaptability to different hand sizes and still manages not to lose much control over the trajectory. The linkage has ambiguous degrees of freedom that are limited when the exoskeleton is attached to the hand, matching the user's natural finger movement. Because the relative proportion of each hand varies significantly less than the absolute proportions, the linkage of each finger was personalized, optimizing the adaptability of the transmission system.

The linkage consists of six bars, with the most proximal bar being a rack that slides on a rail and is also part of the actuation module.

Similar to the attachments, the bars could also be 3D printed. However, the connections of the bars could be made of rivets or strap screws, as these are a cost-effective and resistant solution.

Figure 2: Bar linkage of the transmission module

In terms of adaptability, it is also necessary to adjust the linkage laterally and match it to the central axis of the fingers. Mismatching the transmission module with the fingers would cause deviations from the natural flexion and extension biomechanics and possibly cause discomfort or injury. For this purpose, an adjustable support with a rail (Figure 3) was developed for the rack. The support slides latterly and can be easily fixed and unfixed by tightening and loosening a nut.

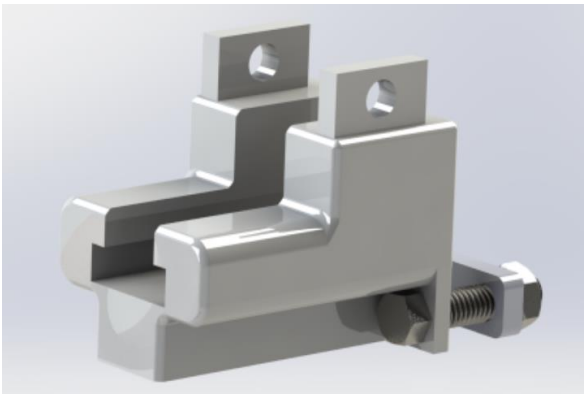

Figure 3: 3D model of the support for the rack and the motor

In addition, the support holds the actuation module. This module consists of a worm mounted on the shaft of a "380:1 Pololu Micro Metal Gearmotor HP 6 V", which transmits rotation to the rack converting it into linear motion. Table 1 shows the technical data of the selected motor.

This mechanical system (Figure 4) provides a compact and less expensive alternative to linear actuators small enough to fit the current application. The worm and rack were resized and modified from a model available online at https://www.mediafire.com/download/lh4zsb1229kf5dq/WormRack2STEP.zip.

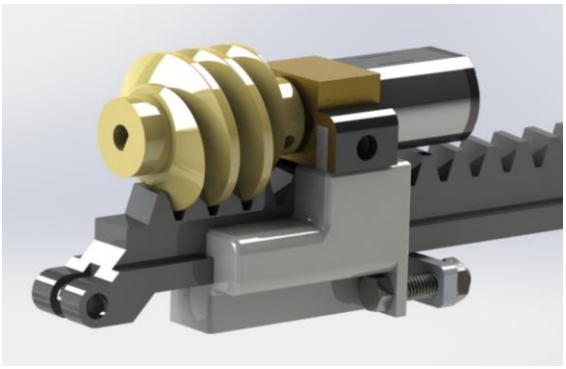

Figure 4: Full actuation module, with support, rack, worm and motor

Table 1
Specifications of the motor at 6V

Specification	Value
No load speed	84 RPM
No load current	0.1 A
Stall Current	1.6 V
Stall Torque	0.54 N.m
Max Output Power	1.1 W

The entire actuation system is encapsulated by the dorsal attachment to prevent injury to the user. Nevertheless, the capsule allows the detachment of the actuation module and the transmission module (through the back) so that the exoskeleton can be adapted and used on either hand by simply reversing the order of these modules.

A set of two 3.7 V (7.4 V total) and 5000 mAh ("radiomaster 5000 mAh 2s li-ion battery pack") batteries power the exoskeleton for a reasonable amount of time, between 5-7 hours of continuous use. A case for the batteries was modeled, which can be attached to the forearm.

Although the control system has not been designed, a basic list of components is proposed for future work and a case for those components has been modeled for visualization purposes:

- arduino Uno
- two “Motoron M3S256 Triple Motor Controller Shield Kits”
- four “Polulu Magnetic Encoder Kits for Metal Gearmotors”

The controllers are stackable and allow a total of six separate motors to be controlled. In addition, the encoders provide position feedback to the controllers. The entire system would be implemented on an Arduino board and powered by the batteries as an external power supply. Alternatively, a custom circuit board could be designed.

Figure 5 shows the overall design of the hand exoskeleton.

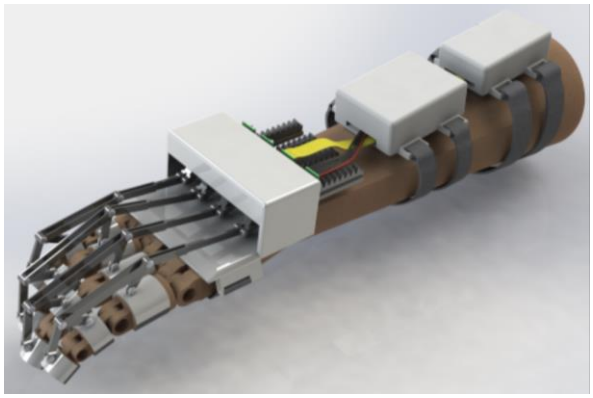

Figure 5: Complete 3D model, with the batteries, control, actuation, and transmission modules.

3. Kinematic analysis

The kinematics of the fingers were validated using the Motion Study feature of Solidworks®, with the Motion Analysis option selected. Contacts were set between the bars, supports and fingers. The motion of the actuation module comes only from mates and no contacts were set. No friction was considered for the contacts and the contact properties were defined as nylon-nylon contact between the bars, nylon-steel(greasy) between the supports and the bars, and steel(greasy)-steel(greasy) between the fingers. Finally, a rotary motion of 80 RPM was set on the worm.

Figure 6 shows the motion of the index finger. The motion of all other fingers was also analyzed, with satisfactory results.

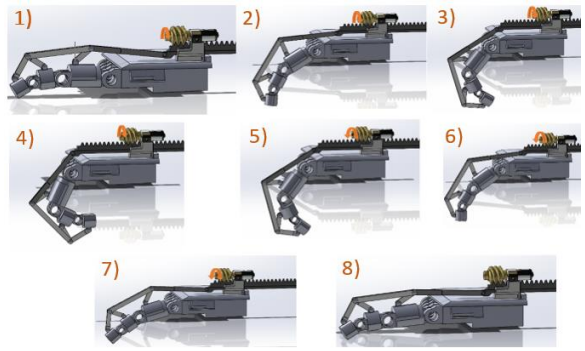

Figure 6: Simulation of the index finger motion, flexion is shown from **1)** to **4)** and extension from **5)** to **8)**

A prototype was built with the same bar dimensions as the model. Even in a situation with different hand sizes, the prototype and the simulation showed similar trajectories (Figure 7), which speaks to both the adaptability of the transmission module and the validity of the simulation.

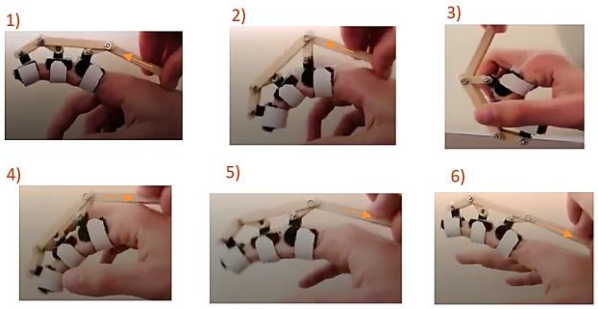

Figure 7: Motion of the index finger with the prototype, flexion is shown from **1)** to **3)** and extension from **4)** to **6)**

The torque required to perform the movement (free movement, unconstrained) never exceeds 0.17 N.mm during flexion (Figure 8-a).

Since gravity acts against the motor during extension, it was included in the study. In extension (Figure 8-b), the effect of gravity can be seen as the finger approaches the plane of action of the rack, as the torque increases with the momentum on the metacarpophalangeal joint. At the maximum extension of the exoskeleton, where the momentum is also maximum, the torque is 0.0009 N.m. (significantly lower than the stall torque of the motor (0.54 N.m).

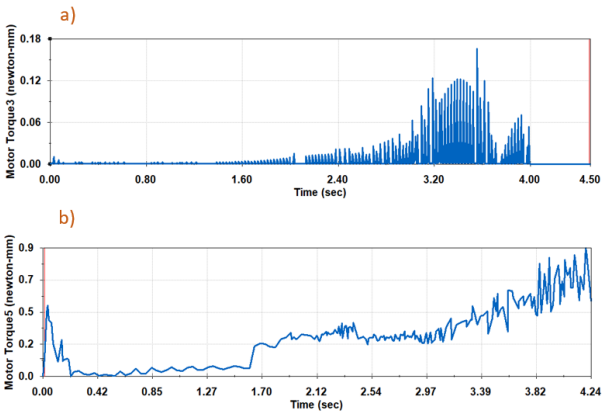

Figure 8: Motor torque during flexion (a) and extension (b)

These results indicate the motor is adequate. Nevertheless, the hand and fingers have a complex force system that was not defined in this simulation and should be gauged with a prototype in the future.

4. Stress Analysis

To find a critical configuration that can be further analyzed with a static study, a structural analysis using motion loads was performed for every bar of the transmission mechanism.

The static study is used to evaluate the stresses when the movement of the hand is hindered by an object in the most critical configuration.

The materials used in the analysis were extruded ABS for the bars (with the average properties from a MatWeb.com database [10], which summarizes all the extruded ABS entries on the website) and Nylon 101 for the rack and worm (with the properties available in Solidworks®).

The properties of ABS and Nylon 101 are listed in Tables 2 and 3, respectively.

Table 2
Properties of ABS

Property	Value
Elastic Modulus	2.06 GPa
Poisson's Ratio	0.393
Mass Density	1080 Kg/m^3
Tensile Strength	38.7 MPa
Yield Strength	40.7 MPa

Table 3
Properties of Nylon

Property	Value
Elastic Modulus	1 GPa
Poisson's Ratio	0.3
Mass Density	1150 Kg/m^3
Tensile Strength	79.29 MPa
Yield Strength	60 MPa

4.1. Structural analysis using motion loads

Following the kinematics analysis, the loads and stresses were evaluated at discrete time steps, to save computational time. There was a time step for every second of the motion, comprising full flexion and extension

In general, the fourth and eighth configurations, corresponding to maximum flexion and extension, were those in which the factor was lower. Nevertheless, in each configuration and for each bar, the factor of safety was always greater than 10^2, thus ensuring the structural integrity of the bars. It is still necessary to evaluate this integrity in a locked configuration and with the motor stall torque acting on the bars.

Since the hand won't be "holding" any object at maximum extension, the fourth configuration was selected for a static study.

4.2. Static analysis

The component interactions between the motor's body and its support and between the worm and the motor's shaft were set to "bonded". In contrast, the interactions between the worm and the rack and between the rack and the support were defined as "contact" (previously "no penetration").

"Pin connectors" with no translation were attached to the finger joints and the bars.

The purpose of the selected component interactions is to evaluate in detail the bars and the rack and the worm, since this are the most critical elements.

Figure 9 shows the four fixtures set on the simulation.

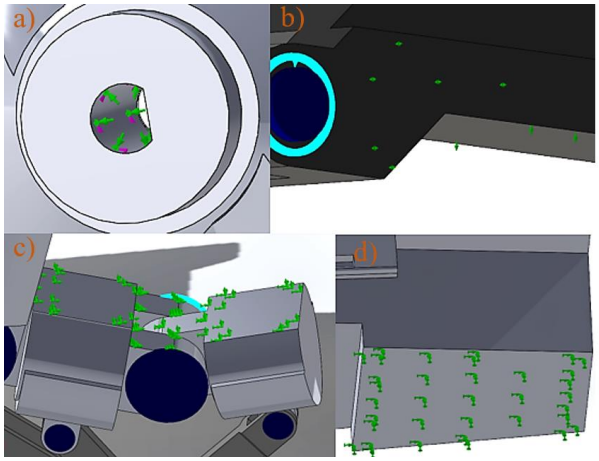

Figure 9: Representation of the fixtures: **a)** a "fixed hinge" fixture in the interior face of the worm. In this type of fixture translational displacement is eliminated and only rotation is considered; **b)** two "roller/slider" fixtures, one on the bottom face of the rack and the other on one of its side faces. This way only displacement along the axis of the rack is allowed, simulating its linear movement; **c)** and **d)** "fixed geometry" fixtures on the volar faces of the intermediate and distal phalanges and on the palm of the hand (as if an object was blocking the movement). These fixtures remove translational displacement

A high-quality mesh of 3D tetrahedral solid elements was created with a mesher from Solidworks®.

Table 4 lists the mesh properties and Figure 10 shows the graphic representation of the mesh.

Table 4
Mesh properties

Property	Value
Mesh type	Solid mesh
Mesher	Blended curvature-based
Jacobian points	16
Max element size	12.0408 mm
Min element size	0.602042 mm
Total nodes	89976
Total elements	51501
% element's aspect ratio < 3	92.9%

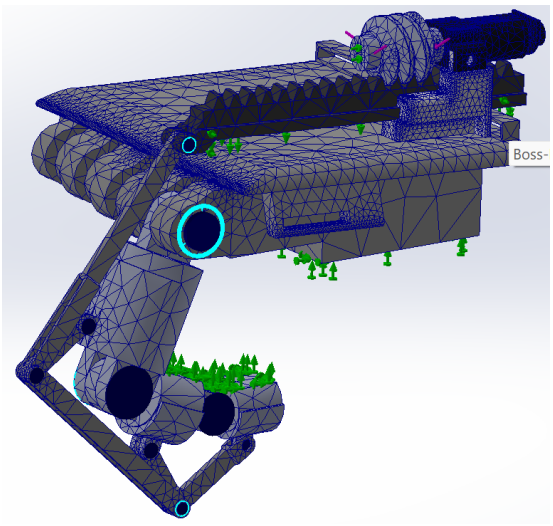

Figure 10: Graphic representation of the high-quality mesh

The factor of safety plot (Figure 11) shows a minimum value of 1.839 occurring on the teeth of the rack. This confirms the need to use Nylon 101, which has a higher yield strength, for the rack and the worm.

The bars have a safety factor always greater than 10. Even though it could be concluded that the transmission mechanism is oversized, unpredictable loads due to accidents or improper use are bound to occur. Therefore, it was considered that the dimensions are feasible and even preferable.

Figure 12 shows the distribution of von Mises stresses along the actuation and transmission modules.

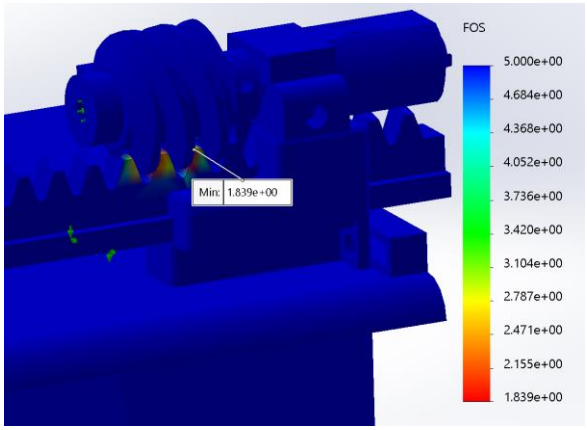

Figure 11: Factor of Safety plot. The minimum factor of safety is located at the teeth contacting the worm

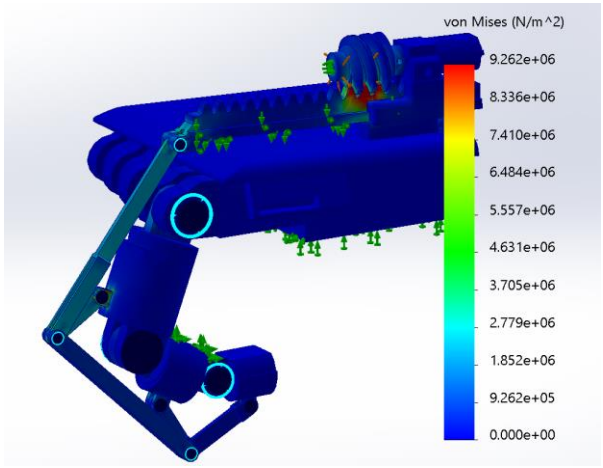

Figure 12: Distribution of von Mises stresses. The biggest stresses happen at the points of contact between the worm and the rack and, in the bars, they decrease from proximal to distal

Finally, the normal forces on the volar surfaces of the fingers show that they can hold objects up to 20 N (Figure 13). The distal phalanx, however, has normal forces opposite to what is expected. This occurs because the mechanism tends to make the distal and intermediate phalanges parallel when flexion continues beyond the maximum point.

This means that when an object rests only on the distal phalanx, the distal phalanx becomes parallel to the intermediate phalanx. However, the hyperextension of the distal phalanx is intentionally limited by the morphology of the bars, and it locks at maximum extension.

Consequently, the load on the object is still indirectly exerted by the intermediate phalanx.

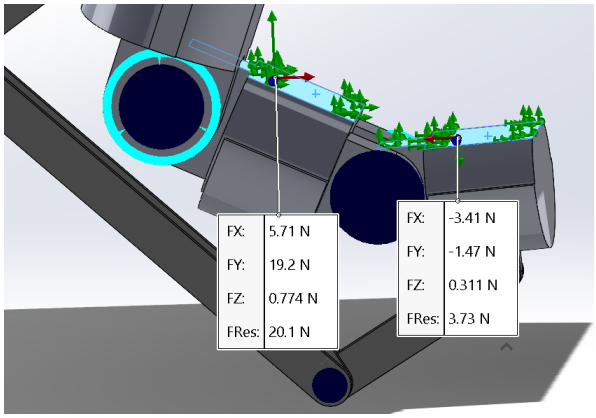

Figure 13: Normal forces on the intermediate and distal phalanges

5. Conclusions

The simulations demonstrate the potential of the exoskeleton as a viable and accessible solution for hand rehabilitation and functionalization. Flexion and extension were achieved in four seconds with a normal force of 20 N at maximum flexion. The trajectory respects the biomechanics of the fingers, which was confirmed with a prototype. When the exoskeleton is maximally flexed in a static study simulating the hand holding an object, the factor of safety is, at its lowest, 1.822.

6. Future Work

In the future, fatigue studies should be performed, especially for the rack and worm. Also, other grips (with different exoskeleton configurations) should be tested in static studies and eventually with a prototype.

The control system will be designed thoroughly and in detail, as will the programming of the exoskeleton. The proposed control elements can manage up to six motors, so a thumb module could be designed and actuated with the remaining two motors.

Force sensors could also be attached to the distal phalanges of the prototype to measure and monitor the progress of the rehabilitation.

7. Acknowledgements

The authors would like to acknowledge the support of the project UIDB/04077/2020.

8. References

[1] American Society of Plastic Surgeons. Plastic surgery statistics report (2020). Available at:https://www.plasticsurgery.org/documents/News/Statistics/2020/plastic-surgery-statistics-full-report-2020.pdf.

[2] E. Bebbington, D. Furniss, "Linear regression analysis of Hospital Episode Statistics predicts a large increase in demand for elective hand surgery in England", Journal of Plastic, Reconstructive & Aesthetic Surgery 68 (2015) 243-251. doi:10.1016/j.bjps.2014.10.011.

[3] D. Carrieri, S. Briscoe, M. Jackson, *et al*, "'Care Under Pressure': a realist review of interventions to tackle doctor's mental ill-health and its impacts on the clinical workforce and patient care", BMJ Open 8 (2018). doi:10.1136/bmjopen-2017-021273.

[4] R. Bos, "Mechanical design of dynamic hand orthoses: Expanding technology with comprehensive overviews and alternative pathways", TUDelft (2019). doi: 10.4233/uuid:011f686f-5f5c-4fc5-9ba5-b613f95abfe2.

[5] B. Hirt, H. Seyhan, M. Wagner, R. Zumhasch, Hand and Wrist Anatomy and Biomechanics: A Comprehensive Guide, Thieme Medical Publishers, 2016.

[6] S. Manna, V. Dubey, "Comparative study of actuation systems for portable upper limb exoskeletons". Medical Engineering & Physics, 60 (2018) 1-13. doi:10.1016/j.medengphy.2018.07.017.

[7] P. Ferguson, Y. Shen, J. Rosen, (2020). "Hand Exoskeleton Systems—Overview", Academic Press. doi:10.1016/B978-0-12-814659-0.00008-4.

[8] T. Du Plessis, K. Djouani, C. Oosthuizen, "A Review of Active Hand Exoskeletons for Rehabilitation and Assistance", Robotics 10 (2021). doi:10.3390/robotics10010040.

[9] T. Greiner, "Hand Anthropometry of U.S. Army Personnel", Army Natick Research Development and Engineering Center MA (1991). Available at: https://apps.dtic.mil/sti/citations/ADA244533.

[10] MatWeb Material Property Data, "Overview of materials for Acrylonitrile Butadiene Styrene (ABS), Extruded". Available at: https://www.matweb.com/search/DataSheet.aspx?MatGUID=3a8afcddac864d4b8f58d40570d2e5aa.